Comparison of Nonlinear Filtering Methods for Battery State of Charge Estimation

A Thesis

Submitted to the Graduate Faculty of the
University of New Orleans
in partial fulfillment of the
requirements for the degree of

Masters of Science
in
Electrical Engineering

by

Klaus Zhang

B.S. Pennsylvania State University, 2011

May 2014

Abstract

In battery management systems, the State of Charge, obtained from voltage and current measurements, is a figure of merit. The estimation of State of Charge is challenging due to the nonlinear behavior of the battery, measurement noise, and the trade-off between accuracy and energy usage in selecting the sample rate. Additionally, for the purposes of eletrical-system design, an electrical-circuit battery model is useful, which presents additional filtering difficulties when compared to presently-used analytical models [wordy]. This thesis investigated the performance of various nonlinear filters for estimating the State of Charge using an electrical-circuit battery model.

Table of Contents

Chapter 1

Introduction

Batteries, particularly rechargeable ones, are used extensively in daily life. They provide the energy for such electrical systems as communication, automotive, and renewable power systems, among others. In order to design for and operate these systems, an accurate battery model and a means of simulating the model efficiently is needed. For example, modern battery charge and health management schemes use high-fidelity battery models to track the state of charge (SOC) and state of health (SOH); this information is then used to predict and optimize runtime of the battery. However, most batteries have nonlinear capacitive effects, which require the use of a nonlinear filter. This thesis provides one possible solution to this problem by choosing an appropriate battery model and testing the speed and accuracy of various nonlinear filters in determining the SOC.

1.1 Electrical Characteristics of Rechargeable Batteries

A high-fidelity battery model has to accurately reproduce the various characteristics of the battery. The characteristics included in most models are the capacity and the state of charge. More accurate models include nonlinear effects, such as the rate-capacity effect and the recovery effect, along with self-discharge and the effects of ambient temperature. The dynamic electrical attributes, such as the current-voltage (i-v) characteristics and transient responses, can also be modeled.

The capacity of a battery is the amount of electric charge it can store, measured in the SI unit Ampere-hours (Ah). Commonly, for rechargeable battery specifications, the subunit milliampere-hour (mAh) is used. Due to the electrochemical nature of batteries, a battery's available capacity decreases as the rate of discharge increases. Therefore, the capacity for a battery is typically stated for a given discharge rate. For lead-acid batteries, this diminishing capacity with increasing discharge rate is known as Peukert's law, which states that for a one-ampere discharge rate [1]

$$C_p = I^k t, \tag{1.1}$$

where C_p is the capacity at a one-ampere discharge rate in Ah, I is the discharge current in A, t is the time to discharge the battery in hours, and $k >= 1$ is the dimensionless Peukert constant, typically between 1.1 and 1.3 for a lead-acid battery. The constant k only equals unity for an ideal accumulator, so for real batteries, k is always greater than unity. Thus, for a given increase in the discharge current, the discharge time decreases by a proportionally greater amount. Therefore, the effective, or available, capacity Ct is reduced. For a general battery, this effect is

known as the rate-capacity effect. Related to this is the recovery effect, so called because when a battery is allowed to rest during an idle period, the battery "recovers" available capacity previously lost during discharge due to the rate-capacity effect.

Both the rate-capacity effect and the recovery effect can be explained by the electrochemical nature of the battery. During discharge the concentration of the active material around the electrode is depleted and the active materials in the depletion region move towards the electrode to reduce the concentration gradient [2]. Because the speed at which the concentration gradient is equalized is limited, the faster the rate of discharge, the less active material has been replenished, resulting in a decrease in the capacity. Likewise, when the battery is allowed to rest, the active material gradient has additional time to equalize and increase the available capacity.

Closely related to the capacity is the SOC. This thesis defines it as the ratio between the remaining capacity and the maximum capacity, with both capacities measured using the amount of active material within the battery. This definition then denotes the proportion of remaining chemical energy rather the available energy and is unaffected by the rate-capacity and recovery effects. Note that a fully charged battery has an SOC of unity and a fully discharged battery has an SOC of zero, regardless of the available capacity. Additionally, it is convenient to establish the relationship between the SOC of the battery and its open-circuit voltage V_{OC}, which is useful for simulation of the i-v characteristics and transient responses. V_{OC} can be thought as the limit of the measured battery voltage after recovery.

Other more minor effects that are usually incorporated into models are self-discharge, the effect of ambient temperature, and aging. Self-discharge refers to an idle battery decreasing its SOC over time due to internal chemical reactions. It is dependent on the type of battery, SOC, ambient temperatures, and other factors.

The ambient temperature has effects on the internal resistance of the battery and the self-discharge rate. Commonly, the battery is designed to operate with a narrow range of temperatures. Below the operating temperature range, the internal resistance increases, decreasing the capacity. Above the operating range, the internal resistance decreases, not only increasing the capacity but also the self-discharge rate; thus, the actual capacity is lowered due to the increased self-discharge. Aging refers to the decrease in battery performance measures, such as capacity, self-discharge, and internal resistance, over time due to unwanted chemical reactions. In practice, aging is indicated by the SOH, defined as the ratio between the current maximum capacity and that of a new battery. The SOH threshold at which the battery performance is considered too degraded varies by application.

[Where does this go?] This thesis studied the prediction of the SOC of a battery using noisy measurements of its current and voltage. To do so accurately for a general load, incorporation of the rate-capacity and recovery effects as well as the transient i-v characteristics is desirable. Furthermore, it is useful to have a model easily tunable for different battery types. The following section reviews the characteristics of different battery models and chooses the one most suitable for the purposes of this study.

1.2 Battery Models

Battery models can be divided into five categories, namely electrochemical, computational intelligence, analytical, stochastic, and electrical-circuit. The remainder of this section reviews each type and determines the most suitable battery model for this study..

1.2.1 Electrochemical

Electrochemical models are describe the chemical processes that place in the battery in great detail. These are generally the most accurate, but they require in-depth knowledge of the chemical processes to create and impose large computational costs [3]. One of the most widely known electrochemical models was developed by Doyle, Fuller, and Newman for lithium and lithium-ion batteries using noninvasive voltage-current cycling experiments [4–6]. It consists of six coupled, nonlinear differential equatons that capture lithium diffusion dynamics and charge transfer kinetics. The model is able to predict i-v response and provides a design guide for thermodynamics, kinetics, and transport across electrodes. A implementation of their model in Fortran, called Dualfoil, is available for free online.[1] The program needs more than 60 parameters along with the load profile in order to compute the battery properties. Setting the parameters requires detailed knowledge of the battery, but the result of the program is highly accurate. Other battery models are often compared to it rather than to experimental results.

1.2.2 Computational Intelligence

Computational intelligence is a brance of computer science interested in problems that require the intelligence of humans and animals to solve. One of the earliest definitions by Bezdek states that computational intelligent systems use pattern recognition on low-level, numerical data and do not use knowledge as with artificial intelligence [8, 9]. Methods such as neural networks, fuzzy systems, and evolutionary computation are commonly classified as computational intelligence. Battery models using such methods as neural networks [10, 11], support vector machines [12],

[1] J. Newman, *Fortran programs for the simulation of electrochemical systems*, `http://www.cchem.berkeley.edu/jsngrp/fortran.html`, 1998.

and hybrid neural-fuzzy models [13] have been studied. These models learn the nonlinear relationships between battery properties, such as SOC, current, voltage, and temperature, through a computationally costly training process. However, once trained, they incur a much lower cost and can achieve comparable accuracy to electrochemical models.

1.2.3 Analytical

[Needs rewrite to include more detail, eg equations]

1.2.3.1 Peukert's Law

Analytical models are simplified electrochemical models that trade off accuracy for simplicity. One of the simplest such models is Peukert's law, described above. It is able to model the rate-capacity effect but not the recovery effect. More complicated models, such as the kinetic battery model and the diffusion model, are able to describe both the rate-capacity effect and the recovery effect. However, the current examples of analytical models cannot describe the transient i-v characteristics of batteries.

1.2.3.2 Kinetic Battery Model

The kinetic battery model (KiBaM), initially created for large lead-acid batteries, describes the battery as a kinetic process, using two charge wells for the bound and available charges connected by a valve whose flow rate is proportional to the height difference between the wells [14].

[Equation that is referenced in the next section.] The change of charge in the

wells is given by

$$\begin{cases} \frac{dy_1}{dt} = -I + k\left(h_2 - h_1\right) \\ \frac{dy_2}{dt} = -k\left(h_2 - h_1\right), \end{cases} \tag{1.2}$$

where y_1, y_2 are the charges, h_1, h_2 are the heights of the wells, the parameter k controls the rate of charge flow between the wells, and I is the applied load.

The flow rate of the valve should be lower than the typical discharge rate of the battery. During discharge from the available-charge well, the bound charges flow through the valve to equalize the heights of the two wells. It can be seen that for slower discharge rates, more charge flows through the valve and the effective capacity increases. Likewise, during idle periods for the battery, the available charge increases. Thus, the model is able to describe the rate-capacity and recovery effects.

1.2.3.3 Diffusion Model

Related to the kinetic battery model is the diffusion model, which describes the movement of the ions in the electrolyte of a lithium-ion battery [15]. Like in the kinetic battery model, the difference in the concentration of adjacent ions along the length of the battery determines the diffusion rate of the ions. The available charges are those ions directly touching the electrode of the battery. It can be seen that the kinetic battery model is a first-order approximation of the diffusion model [3], so naturally the diffusion model also describes the rate-capacity and recovery effects.

1.2.4 Stochastic

Stochastic models describe the discharging and the recovery effect as stochastic processes. The first models were developed by Chiasserini and Rao and based on discrete-time Markov chains [16]. They studied two models of a battery in a commu-

nication device that transmitted packets. The simpler model described the battery as a discrete-time Markov chain with $N + 1$ states, numbered from 0 to N and corresponding to the number of charge units available in the battery. Transmitting one packet requires one charge unit of energy. Thus, in continuous transmission, N packets can be sent. At every time step, a charge unit is either consumed with probability $a_1 = q$ or recovered with probability $a_0 = 1 - q$. The battery is considered empty when the 0 state is reached or when a theoretical maximum of T charge units have been consumed. The second model is an extension of the first, allowing for more than one charge unit to be consumed in a time step, modeling more bursty usage. Additionally, the battery has a non-zero probability of staying in the same charge state, indicating no consumption or recovery during a time step. Chiasserini and Rao extended their model further in following papers by adding state and phase dependence [2, 17, 18]. The state number is the number of charge units, and the phase number is the number of consumed charge units. Having fewer charge units decreases the probability of recovery, while having more consumed charge units increases the probability of recover. Using these models, one can model different loads by setting the transitions probabilities. However, the order of the transitions is uncontrollable, so it is impossible to model fixed load patterns and compute their impact on battery life.

Chiasserini and Rao mainly investigated the gain G in transmitted packets using a pulsed discharge relative to using a constant discharge, defined as $G = m/N$, where m is the mean number of transmitted packets. The gain increases when the load decreases, due to an increase in the recovery probability. Additionally, the gain increases for lower discharge demand rates and higher current densities. These load profiles result in discharge currents close to the specified limits of the battery, causing the available capacity to decrease overly quickly. Therefore, the recovery

effect is especially strong for these cases during pulsed discharge, greatly increasing the gain. Chiasserini and Rao compared the computation of the gain parameter for different current densities and demand rates using the stochastic model to that of the electrochemical model of Doyle et al. They found an average deviation of 1% and a maximum deviation of 4%. This shows that the stochastic model accurately describes battery behavior during pulsed discharge. However, this model is only able to compute relative lifetimes.

In 2005, Rao et al. [19] proposed a stochastic battery model based on the Kinetic Battery Model (KiBaM) of Manwell and McGowan. This stochastic KiBaM was for a nickel-metal hydride (NiMH) battery. The differential equations governing the original KiBaM were modified to include an extra factor h_2 governing the flow of charge between the wells. This changes Eq. (1.2) into

$$\begin{cases} \frac{dy_1}{dt} = -I + k_s h_2 \left(h_2 - h_1\right) \\ \frac{dy_2}{dt} = -k_s h_2 \left(h_2 - h_1\right), \end{cases} \tag{1.3}$$

This change causes the recovery effect to weaken as the remaining charge decreases. The stochastic model was also modified to allow the possibility of no recovery during idle periods. The stochastic KiBaM describes the battery using a discrete-time, transient Markov process. The states are labeled with the parameters (i, j, t), with i and j representing the discrete charge levels of the available and bound charge wells and t representing the length of the current idle period. Like the stochastic model of Chiasserini and Rao, it is impossible to fully model a real-life discharge pattern using the stochastic KiBaM. Rao et al. compared the results of their model with experimental results using an AAA NiMH battery. Two sets of experiments were conducted, the first with varying frequency of the load and a 50% duty cycle and

the second with varying off-time and a constant on-time. Their model accurately predicted the lifetime and delivered charge from the battery, with a maximum error of 2.65%.

1.2.5 Electrical-Circuit

Electrical-circuit models for batteries developed from the discovery of capacitative effects at the electrode-electrolyte interface. Helmholtz first proposed the existence of a double layer of charge at the interface in 1879. In 1899, Warburg proposed a series resistance and capacitance circuit model with an infinitely low current density. The Warburg capacitance C_W named after him varies inversely with the square root of the frequency [20]. In 1947, Randles proposed a model consisting of a double-layer polarization capacitance C_p in parallel with the series combination of a resistor R and a capacitance C [21]. In 1994, Kovacs improved Randles circuit with the addition of Warburg impedence Z_W replacing the capacitance C and the solution resistance R_s in series with the original Randles circuit [22]. In addition, he renamed C_p to the double layer capacitance C_{dl} and R to the charge-transfer resistance R_{ct}. These proposals came from a desire to represnt impedance spectra created using electrochemical impedance spectroscopy (EIS). The various elements in the models represent the different processes within a battery, which have different time constants. While these attempts model the impedance and, thus, account for the nonlinear rate-capacity and recovery effects, they do not consider the capacity and self-discharge of the battery.

In 1993, Hageman created simplified electrical-circuit models using PSpice for nickel-cadmium (NiCd), lead-acid, and alkaline batteries [23]. The circuits shared the common elements of *i*) a capacitor that represents the battery capacity, *ii*) a

discharge rate normalizer that determines the additional capacity loss at high discharge rates, *iii*) a circuit that discharges the battery, *iv*) a lookup table of battery voltage versus SOC, and *v*) a resistor that represents the battery's internal resistance [23, 24]. In addition, battery models for NiCd batteries simulated the thermal effects under high discharge rates. The main lookup table is formed by discharging a battery at a low rate at a constant current (20 to 200 hours). At high discharge rates, the discharge rate normalizer reduces the battery voltage below the value from looking up the SOC in the table. This normalizer is implemented using additional lookup tables. These circuit models are much simpler than electrochemical models, but they are also less accurate with an approximate error of 10%. Furthermore, creation of the lookup tables requires considerable data. These circuit-based models are mainly concerned with modeling the remaining discharge time and are referred to as runtime-based models.

In 2006, Chen and Rincón-Mora proposed a combination of a runtime-based model and a impedance-based model consisting of a series resistor and two parallel resistor-capacitor networks [25]. The elements of the impedance part of the model had parameters that depended on the SOC. Additionally, the runtime model included a resistance that modeled the self-discharge rate. Their proposed model has the advantage of accurate prediction of the SOC using the runtime-based portion while also modeling nonlinear transient effects, such as the rate-capacity and recover effects, with the impedance-based portion. Furthermore, the battery data can be collected using EIS measurements, which requires neither detailed knowledge of the battery chemistry nor lengthy, low-rate discharge experiments.

1.2.6 Evaluation

Of the model types, only some are fit for use with filtering algorithms. The computational-intelligence and stochastic models do not model the dyanmics of the battery system, so they cannot be used. The electrochemical models, the related analytical models, and the electrical-circuit models describe the system dynamics and the nonlinear rate-capacity and recovery effects. However, only the electrical-circuit model has the advantage of modeling the internal impedance of the battery, which is useful in the design of battery systems. Of the electrical-circuit models, the proposal by Chen and Rincón-Mora is best suited for the purposes of this thesis since it is the only one discussed by this paper that describes both the capacity and the transient effects. Therefore, their proposal is used for the simulation of the battery and comparing the performance of different filters.

1.3 Nonlinear Filtering Methods

The battery model chosen for the purposes of this thesis has the advantage that it can be written in state-space form for use with commonly available state space filters. The rest of this section discusses the various nonlinear filtering techniques that can be applied to the model.

Chapter 2

Methodology

2.1 Battery Model

As discussed in the previous section, this thesis considers the electrical-circuit battery model proposed by Chen and Rincón-Mora [25] and shown in Figure 2.1. The left portion of the circuit models the capacity, SOC, and runtime, while the right portion models the transient i-v characteristics. For convenience, the model is designed so that the SOC of the battery equals the voltage V_{SOC}, in volts. The parameters C_{cap} and R_{sd} are assumed constant for a given battery and determine the capacity and self-discharge rate of the battery. The other parameters are all nonlinear functions of V_{SOC} and determine the transient i-v response as well as the open-circuit voltage V_{OC}. From a typical TCL PL-383562 polymer lithium-ion battery, Chen and Rincón-Mora extracted these parameters and fit them to curves, obtaining

$$R_s(V_{\mathrm{SOC}}) = 0.1562e^{-24.37V_{\mathrm{SOC}}} + 0.07446 \tag{2.1}$$

$$R_{ts}(V_{\mathrm{SOC}}) = 0.3208e^{-29.14V_{\mathrm{SOC}}} + 0.04669 \tag{2.2}$$

$$C_{ts}(V_{\mathrm{SOC}}) = -752.9e^{-13.51V_{\mathrm{SOC}}} + 703.6 \tag{2.3}$$

$$R_{tl}(V_{\mathrm{SOC}}) = 6.603e^{-155.2V_{\mathrm{SOC}}} + 0.04984 \tag{2.4}$$

$$C_{tl}(V_{\mathrm{SOC}}) = -6056e^{-27.12V_{\mathrm{SOC}}} + 4475 \tag{2.5}$$

$$V_{\mathrm{OC}}(V_{\mathrm{SOC}}) = -1.031e^{-35V_{\mathrm{SOC}}} + 3.685 + 0.2156V_{\mathrm{SOC}} - 0.1178V_{\mathrm{SOC}}^2 + 0.3201V_{\mathrm{SOC}}^3 \tag{2.6}$$

The resistance and capacitance parameters shown above are approximately constant for SOC > 0.2 and change exponentially for SOC < 0.2. The open-circuit voltage also changes exponentially for SOC < 0.2 but is approximately linear for SOC > 0.2. Note that the capacitances C_{ts} and C_{tl} are negative for SOC values close to zero, which is both unrealistic according to the experimental data collected by Chen and Rinón-Mora and problematic mathematically. To solve this, a lower bound was placed on the V_{SOC} input to the capacitance functions. Thus, for inputs below some threshold value v_T, the capacitances are adjusted to their value at that threshold, producing

$$\hat{C}_{ts}(V_{\mathrm{SOC}}) = \begin{cases} C_{ts}(V_{\mathrm{SOC}}), & V_{\mathrm{SOC}} \geq v_T \\ C_{ts}(v_T), & V_{\mathrm{SOC}} < v_T \end{cases} \tag{2.7}$$

$$\hat{C}_{tl}(V_{\mathrm{SOC}}) = \begin{cases} C_{tl}(V_{\mathrm{SOC}}), & V_{\mathrm{SOC}} \geq v_T \\ C_{tl}(v_T), & V_{\mathrm{SOC}} < v_T \end{cases} \tag{2.8}$$

The threshold v_T was chosen based on the experimental data of Chen and Rinón-Mora, specifically so that the threshold capacitance values are approximately equal to the lowest such values measured by them. A threshold of $v_T = 0.015$ V accomplishes this goal.

This study used the nonlinear parameters given by Chen and Rincón-Mora for

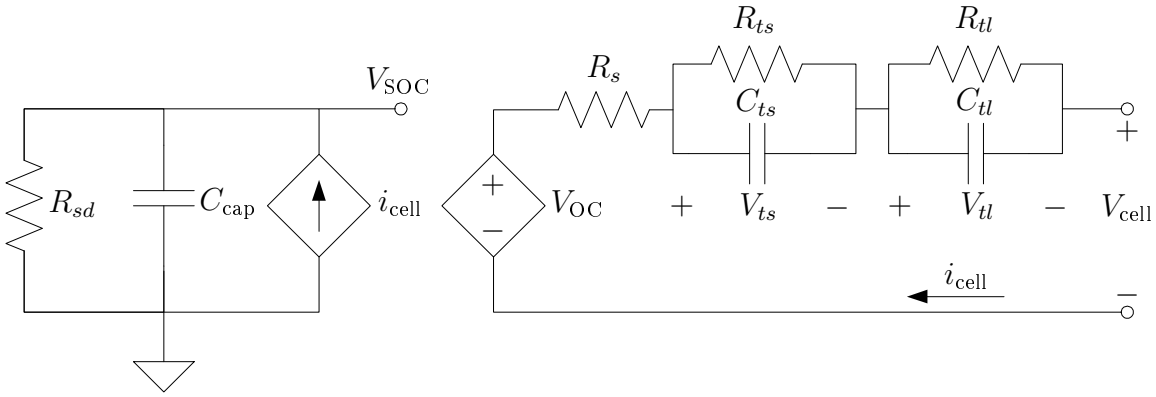

Figure 2.1: Electrical-circuit battery model.

the implementation of a battery using their battery model in Matlab. In addition, the thresholding defined in Eqs. (2.7) and (2.8) was used with $v_T = 0.015$ V. The other, constant parameters were chosen to produce a capacity of 1 Ah and a self-discharge rate of 4% per month. To do so, the capacitance $C_{\rm cap}$ is calculated to hold the desired capacity when $V_{\rm SOC} = 1$ V, and then the resistance R_{sd} is set to produce the desired self-discharge rate. For a given capacity of $C^\dagger$ in Ah, $C_{\rm cap}$ needs to be

$$C_{\rm cap} = \frac{Q}{V_{\rm SOC}} = \frac{C^\dagger}{1\ \text{V}} = 3600 C^\dagger\ [\text{F}]. \tag{2.9}$$

Then, the resistance R_{sd} is chosen so that the time constant $\tau = RC$ results in the desired drop of $\xi = 0.04$ over $T = 1$ month as follows

$$V(t) = V_0 e^{-T/\tau} = V_0(1-\xi) \tag{2.10}$$

$$\tau = -T/\ln(1-\xi) = -2592000/\ln 0.96\ [\text{s}]. \tag{2.11}$$

Then, $R_{sd} = \tau / C_{\rm cap}$. Thus, the parameters are $C_{\rm cap} = 3600$ F and $R_{sd} = 17.6376\ \text{k}\Omega$.

In order to simulate the use of the modeled battery, discharging and charging loads were implemented, as shown in Figures 2.2. For discharging, a resistive load

R_L is placed across the battery terminals, creating a discharge rate of $i_{\text{cell}} = V_{\text{cell}}/R_L$. For charging, a negative resistance $-R_L$, where $R_L > 0$, is used, creating a charging current of $-i_{\text{cell}} = V_{\text{cell}}/R_L$. Thus, any arbitrary charging or discharging current can be set by choosing the appropriate resistance R_L. Furthermore, an open circuit can be simulated by choosing R_L sufficiently large so that $i_{\text{cell}} \approx 0$. Additional consideration has to be taken to produce constant current and constant voltage charging conditions for standard charging procedure. Typically, the specific battery modeled by the given parameters is charged at a rate of $C_5/5$ until a terminal voltage of 4.2 V is reached, where $C_5/5$ is the discharge rate at which a full battery is completely discharged in 5 hours. Then, the battery is charged at a constant voltage of 4.2 V until the charging current is below $C_5/20$. The constant current condition is met by varying R_L so that V_{cell}/R_L stays constant, while the constant voltage condition is met by varying R_L so that $i_{\text{cell}}R_L$ stays constant.

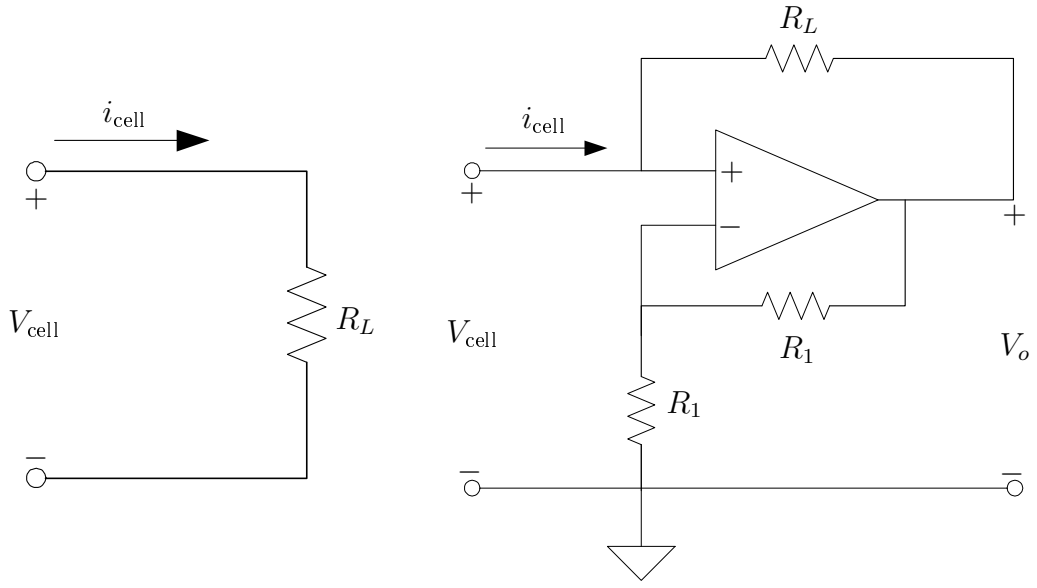

Figure 2.2: Loads to (a) discharge and (b) charge the battery.

This use of the load R_L to control the current i_{cell} suggests that it is the input to the system. Moreover, the outputs of the system are V_{cell} and i_{cell}. However, since

knowledge of one of them along with R_L allows for the calculation of the other, the two outputs have a known relationship between them. Therefore, only one of the outputs is necessary to fully define the input-output relationship of the system. In this study, the voltage V_{cell} was chosen as the output.

For ease of numerical simulation, it is useful to find the state-space system for the circuit. The state-space representation is derived using the physical variable definition, in which the state variables are chosen to represent the voltages across the capacitors. Choosing $x_1 = V_{\text{SOC}}$, $x_2 = V_{ts}$, and $x_3 = V_{tl}$ achieves this goal and results in the state-space representation

$$\dot{x}_1 = -\frac{x_1}{R_{sd}C_{\text{cap}}} - \frac{V_{\text{OC}}(x_1) - x_2 - x_3}{(R_s(x_1) + R_L)C_{\text{cap}}} + f_{w,1}(\mathbf{x}, R_L, \mathbf{w}) \tag{2.12}$$

$$\dot{x}_2 = -\frac{x_2}{R_{ts}(x_1)C_{ts}(x_1)} + \frac{V_{\text{OC}}(x_1) - x_2 - x_3}{(R_s(x_1) + R_L)C_{ts}(x_1)} + f_{w,2}(\mathbf{x}, R_L, \mathbf{w}) \tag{2.13}$$

$$\dot{x}_3 = -\frac{x_3}{R_{tl}(x_1)C_{tl}(x_1)} + \frac{V_{\text{OC}}(x_1) - x_2 - x_3}{(R_s(x_1) + R_L)C_{tl}(x_1)} + f_{w,3}(\mathbf{x}, R_L, \mathbf{w}) \tag{2.14}$$

$$V_{\text{cell}} = \frac{V_{\text{OC}}(x_1) - x_2 - x_3}{1 + R_s(x_1)/R_L} + f_v(\mathbf{x}, R_L, \mathbf{v}), \tag{2.15}$$

where R_L is the input to the system, V_{cell} is the output, f_w is the process noise function, f_v is the measurement noise function, and the nonlinear parameters depending on x_1 are given by Eqs. (2.1) through (2.6) along with the thresholding defined in Eqs. (2.7) and (2.8). It is obvious from this formulation that the system is nonlinear to both the input and the states. In order to establish the noise expressions, the types of noise present in the battery have to first be determined.

This thesis assumes that the process and measurement noises in this system are due to thermal noise in the resistances for the internal impedance of the battery R_s, R_{ts}, and R_{tl}, and for the load R_L. This is motivated by measurements of the voltage noise in batteries conducted by Boggs et al. that showed the measured noise is mainly

due to thermal noise; the correlation between the battery terminals suppresses shot noise [26]. This thermal noise is assumed to be Gaussian white noise with a power spectral density (PSD) of [27]

$$S_n(\omega) \cong 2kT \text{ watts per Hz} \qquad \text{for} \qquad |\omega| \ll 2\pi kT/h, \tag{2.16}$$

where T is the temperature of the conducting medium in Kelvin, k is the Boltzmann's constant, and h is the Planck's constant. Figure 2.3 shows that the thermal noise due to the resistances is modeled as voltage sources in series with the resistances, with PSDs of $S_v(\omega) = 2kTR$ for a corresponding resistance R. Using this definition, the noise functions are given by

$$f_{w,1} = \frac{v_{n_s} + v_{n_L}}{(R_s(x_1) + R_L)C_{\text{cap}}} \tag{2.17}$$

$$f_{w,2} = \frac{v_{n_{ts}}}{R_{ts}(x_1)C_{ts}(x_1)} - \frac{v_{n_s} + v_{n_L}}{(R_s(x_1) + R_L)C_{ts}(x_1)} \tag{2.18}$$

$$f_{w,3} = \frac{v_{n_{tl}}}{R_{tl}(x_1)C_{tl}(x_1)} - \frac{v_{n_s} + v_{n_L}}{(R_s(x_1) + R_L)C_{tl}(x_1)} \tag{2.19}$$

$$f_v = -\frac{v_{n_s} + v_{n_L}}{1 + R_s(x_1)/R_L}. \tag{2.20}$$

It can be seen that the resistances change over time, which causes the covariance of the sources v_n to also change. For the purposes of modeling, it is useful to define noise variables that have constant covariance. Using the square root of the power supplied by the noise sources as the noise variables accomplishes this goal and produces the variables $w_1 = v_{n_s}/\sqrt{R_s}$, $w_2 = v_{n_{ts}}/\sqrt{R_{ts}}$, $w_3 = v_{n_{tl}}/\sqrt{R_{tl}}$, and $w_4 = v_{n_L}/\sqrt{R_L}$, which all have constant covariances of $2kT$. Then, the state space

representation of the system becomes

$$\dot{x}_1 = -\frac{x_1}{R_{sd}C_{\text{cap}}} - \frac{V_{\text{OC}}(x_1) - x_2 - x_3 - \sqrt{R_s(x_1)}w_1 - \sqrt{R_L}w_4}{(R_s(x_1) + R_L)C_{\text{cap}}} \tag{2.21}$$

$$\dot{x}_2 = -\frac{x_2 - \sqrt{R_{ts}(x_1)}w_2}{R_{ts}(x_1)C_{ts}(x_1)} + \frac{V_{\text{OC}}(x_1) - x_2 - x_3 - \sqrt{R_s(x_1)}w_1 - \sqrt{R_L}w_4}{(R_s(x_1) + R_L)C_{ts}(x_1)} \tag{2.22}$$

$$\dot{x}_3 = -\frac{x_3 - \sqrt{R_{tl}(x_1)}w_3}{R_{tl}(x_1)C_{tl}(x_1)} + \frac{V_{\text{OC}}(x_1) - x_2 - x_3 - \sqrt{R_s(x_1)}w_1 - \sqrt{R_L}w_4}{(R_s(x_1) + R_L)C_{tl}(x_1)} \tag{2.23}$$

$$V_{\text{cell}} = \frac{V_{\text{OC}}(x_1) - x_2 - x_3 - \sqrt{R_s(x_1)}w_1 - \sqrt{R_L}w_4}{1 + R_s(x_1)/R_L}. \tag{2.24}$$

This thesis assumed that a standard temperature of $T = 290$ Kelvin. Therefore, the noise variables have covariances of $\sigma^2 = 2kT = 8.0078 \times 10^{-21}$ W/Hz.

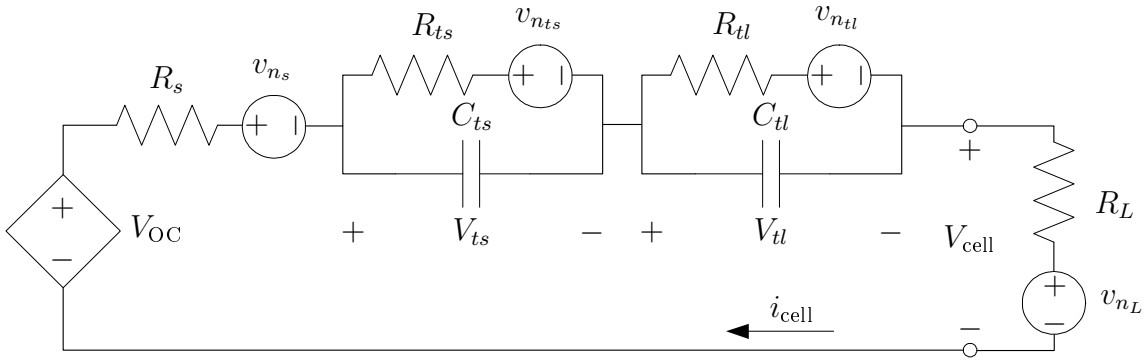

Figure 2.3: Modeling of thermal noise in resistances as voltage sources in series with the resistances.

2.2 Simulation Setup

In order to generate the input and output of the system, the battery model was implemented in Simulink. Figure 2.4 shows a simulation of the battery, assuming no noise, discharged with $R_L = 5\ \Omega$ from 5 to 120 minutes and charged with $R_L = -5\ \Omega$ from 150 to 250 minutes. A mechanism was implemented that bounded the SOC

to $0 \leq \text{SOC} \leq 1$, which can be seen in i_{cell}. Figure 2.5 shows a simulation with the same input, assuming thermal noise. It can be seen that the effect of noise is minimal. This is better seen in Figure 2.6, which shows the squared difference between the outputs of the noiseless and noisy systems.

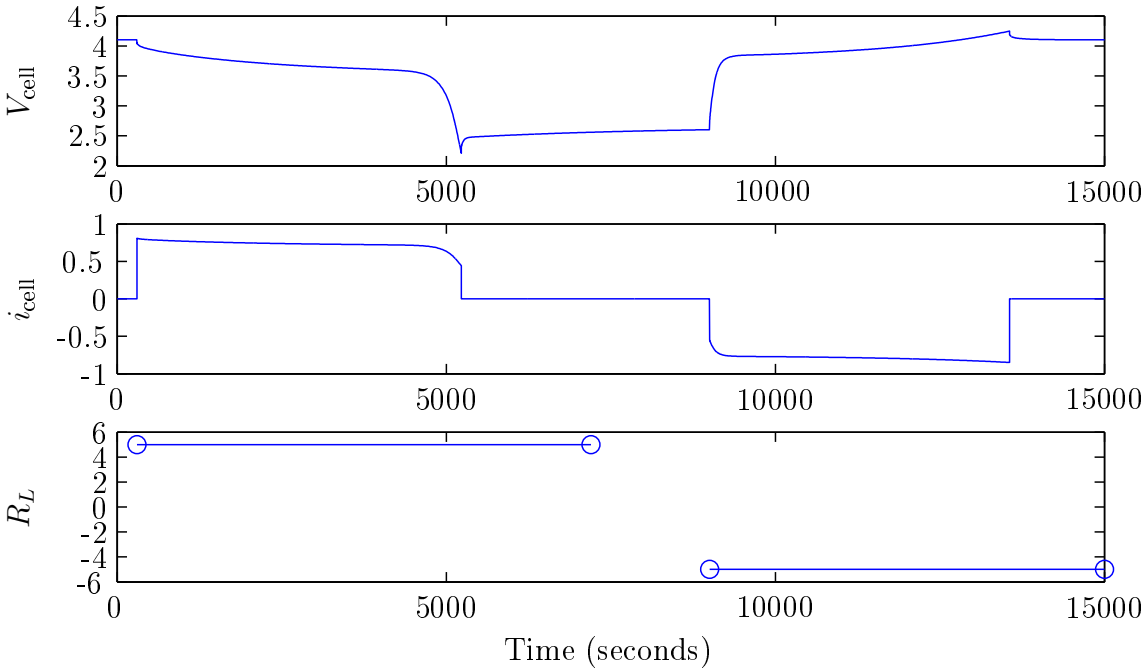

Figure 2.4: Test of discharging battery with resistive load and charging using negative resistance assuming no noise.

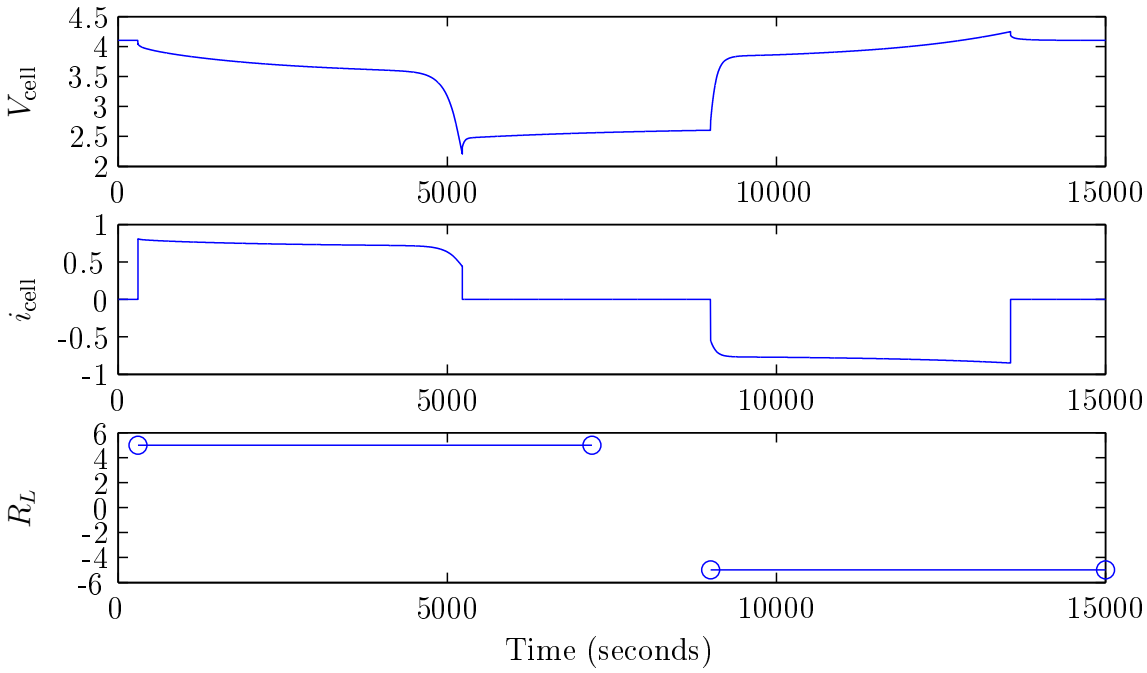

Figure 2.5: Test of discharging battery with resistive load and charging using negative resistance assuming thermal noise.

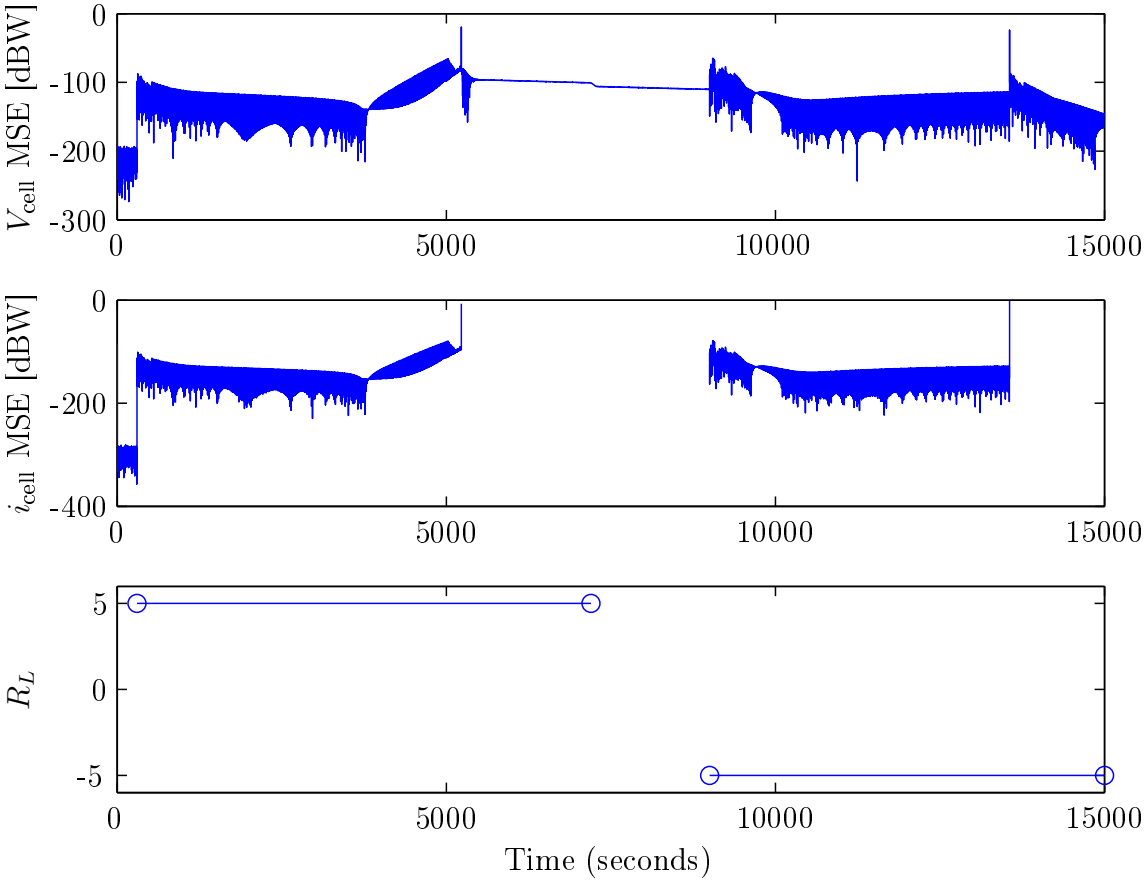

Figure 2.6: Comparison of outputs between noiseless and noisy systems.

2.3 Filter Implementations

Bibliography

[1] D. Doerffel and S. A. Sharkh, "A critical review of using the peukert equation for determining the remaining capacity of lead-acid and lithium-ion batteries," *Journal of Power Sources*, vol. 155, no. 2, pp. 395–400, 2006.

[2] C. F. Chiasserini and R. R. Rao, "A model for battery pulsed discharge with recovery effect," in *Wireless Communications and Networking Conference, 1999. WCNC. 1999 IEEE*, vol. 2, 1999, pp. 636–639.

[3] M. R. Jongerden and B. R. Haverkort, "Which battery model to use?" *IET Software*, vol. 3, no. 6, pp. 445–457, Dec. 2009.

[4] M. Doyle, T. F. Fuller, and J. Newman, "Modeling of galvanostatic charge and discharge of the lithium/polymer/insertion cell," *Journal of the Electrochemical Society*, vol. 140, no. 6, pp. 1526–1533, 1993.

[5] T. F. Fuller, M. Doyle, and J. Newman, "Simulation and optimization of the dual lithium ion insertion cell," *Journal of the Electrochemical Society*, vol. 141, no. 1, pp. 1–10, 1994.

[6] ——, "Relaxation phenomena in lithium-ion insertion cells," *Journal of the Electrochemical Society*, vol. 141, no. 4, pp. 982–990, 1994.

[7] J. Newman, *Fortran programs for the simulation of electrochemical systems*, `http://www.cchem.berkeley.edu/jsngrp/fortran.html`, 1998.

[8] J. C. Bezdek, "On the relationship between neural networks, pattern recognition and intelligence," *International Journal of Approximate Reasoning*, vol. 6, no. 2, pp. 85–107, 1992.

[9] ——, "What is computational intelligence?" In *Computational Intelligence: Imitating Life*, J. M. Zurada, R. J. Marks, and C. J. Robinson, Eds., IEEE Press, 1994, pp. 1–12.

[10] C. C. O'Gorman, D. Ingersoll, R. G. Jungst, and T. L. Paez, "Artificial neural network simulation of battery performance," in *Proceedings of the Thirty-First Hawaii International Conference on System Sciences*, vol. 5, Jan. 1998, pp. 115–121.

[11] G. Capizzi, F. Bonanno, and G. M. Tina, "Recurrent neural network-based modeling and simulation of lead-acid batteries charge-discharge," *IEEE Transactions on Energy Conversion*, vol. 26, no. 2, pp. 435–443, Jun. 2011.

[12] J. Wang, Q. Chen, and B. Cao, "Support vector machine based battery model for electric vehicles," *Energy Conversion and Management*, vol. 47, no. 7–8, pp. 858–864, 2006.

[13] W. X. Shen, C. C. Chan, E. W. C. Lo, and K. T. Chau, "Adaptive neuro-fuzzy modeling of battery residual capacity for electric vehicles," *IEEE Transactions on Industrial Electronics*, vol. 49, no. 3, pp. 677–684, Jun. 2002.

[14] J. F. Manwell and J. G. McGowan, "Lead acid battery storage model for hybrid energy system," *Solar Energy*, vol. 50, no. 5, pp. 399–405, 1993.

[15] D. N. Rakhmatov and S. B. K. Vrudhula, "An analytical high-level battery model for use in energy management of portable electronic systems," in *Proceedings of the 2001 IEEE/ACM International Conference on Computer-aided Design*, ser. ICCAD '01, San Jose, California: IEEE Press, 2001, pp. 488–493.

[16] C. F. Chiasserini and R. R. Rao, "Pulsed battery discharge in communication devices," in *Proceedings of the 5th Annual ACM/IEEE International Conference on Mobile Computing and Networking*, ser. MobiCom '99, 1999, pp. 88–95.

[17] ——, "Improving battery performance by using traffic shaping techniques," *IEEE Journal on Selected Areas in Communications*, vol. 19, no. 7, pp. 1385–1394, 2001.

[18] ——, "Energy efficient battery management," *IEEE Journal on Selected Areas in Communications*, vol. 19, no. 7, pp. 1235–1245, 2001.

[19] V. Rao, G. Singhal, A. Kumar, and N. Navet, "Battery model for embedded systems," in *Proceedings of the 18th International Conference on VLSI Design held jointly with 4th International Conference on Embedded Systems Design*, ser. VLSID '05, Washington, DC, USA: IEEE Computer Society, 2005, pp. 105–110.

[20] L. A. Geddes, "Historical evolution of circuit models for the electrode-electrolyte interface," *Annals of Biomedical Engineering*, vol. 25, no. 1, pp. 1–14, 1997. [Online]. Available: `http://dx.doi.org/10.1007/BF02738534`.

[21] J. E. B. Randles, "Kinetics of rapid electrode reactions," *Discussions of the Faraday Society*, vol. 1, pp. 11–19, 1947.

[22] G. T. A. Kovacs, "Introduction to the theory, design, and modeling of thin-film microelectrodes for neural interfaces," in *Enabling Technologies for Cultured Neural Networks*, D. A. Stenger and T. M. McKenna, Eds., New York: Academic Press, 1994, ch. 7.

[23] S. C. Hageman, "Simple PSpice models let you simulate common battery types," *Electronic Design News*, vol. 38, pp. 117–129, 1993.

[24] ——, "Using PSpice to simulate the discharge behavior of common batteries," in *MicroSim Application Notes*, ver. 8.0, MicroSim Corporation, 1997, pp. 260–286.

[25] M. Chen and G. A. Rincón-Mora, "Accurate electrical battery model capable of predicting runtime and i-v performance," *IEEE Transactions on Energy Conversion*, vol. 21, no. 2, pp. 504–511, Jun. 2006.

[26] C. K. Boggs, A. D. Doak, and F. L. Walls, "Measurement of voltage noise in chemical batteries," in *Proceedings of the 49th IEEE International Frequency Control Symposium*, May 1995, pp. 367–373.

[27] F. G. Stremler, *Introduction to Communication Systems*, 2nd ed. Reading, MA: Addison-Wesley, 1982.